- Home
- Registration
- Call for Papers
- Paper Submission
- Organizing Committee
- Technical Program Committee
- Keynote Lectures
- Panel Session
- Conference Program
- Awards
- Past ICCAs

Technical Sponsor

IEEE CONTROL SYSTEMS SOCIETY

Organizer

IEEE CSS Chapter

IEEE Control Systems Chapter, Singapore

The 16th IEEE International Conference on Control and Automation

IEEE ICCA 2020 – www.ieee-icca.org

Plenary Panel Session

Autonomous Systems, AI and Commercialization Opportunities

Time: 10:00–11:40am, October 11, 2020 (Singapore/Beijing/Hong Kong time), Sunday
10:00–11:40pm, October 10, 2020 (New York/Washington DC time), Saturday
07:00–08:40pm, October 10, 2020 (Vancouver/San Francisco time), Saturday

Venue: Zoom Meeting: https://cuhk.zoom.us/j/97039359394(ID: 970 3935 9394)
(Tencent meeting platform users, please refer to the web link appended at the end)

Chairs: Professor Jie Chen, Tongji University & Beijing Institute of Technology, China
Professor Ben M. Chen, Chinese Univ. of Hong Kong & National University of Singapore

Panelists: Professor Clarence W. de Silva, University of British Columbia, Canada
Professor Wei Kang, Naval Postgraduate School, USA
Professor Tong Boon Quek, Ministry of Trade and Industry, Singapore
Professor Yacov A. Shamash, Stony Brook University, USA
Professor Bin Xin, Beijing Institute of Technology, China

The theme of the IEEE ICCA plenary session this year is Autonomous Systems, AI and Commercialization Opportunities. We are honored that five prominent experts and educators in the field will join this panel to share their expertise and visions, and to discuss challenges in autonomous systems research issues and business opportunities. Through direct dialog with these world-renowned panelists, we aim to gain a deeper insight into some fundamental and emerging problems in autonomous systems and a broader picture on their commercialization potentials.

This panel will also serve as a platform for exchanging ideas and debating general issues in control and automation. It offers an opportunity too for the audience, in particular students and junior researchers, to hear the opinions of senior members of our community on issues we often face at the early stage of our career or study

We introduce our panelists in the alphabetic order.

Professor Clarence W. de Silva has been a Professor of Mechanical Engineering at University of British Columbia, Vancouver, Canada, since 1988. He received Ph.D. degrees from Massachusetts Institute of Technology and the University of Cambridge, U.K., honorary D.Eng. degree from University of Waterloo, Canada, and the higher doctorate (ScD) from University of Cambridge.

Professor de Silva is a Fellow of IEEE, ASME, Canadian Academy of Engineering, and Royal Society of Canada. Also, he has been a Senior Canada Research Chair, NSERC-BC Packers Chair in Industrial Automation, Mobil Endowed Chair, Lilly

17:00-18:30	**Session SatC3 - Learning System & Optimal Control 1** Papers: 51, 59, 107, 171, 178, 356 (https://ntu-sg.zoom.us/j/94109310417)	**Session SatC4 - Distributed Optimization and Learning** Papers: 103, 160, 214, 332, 387 (https://ntu-sg.zoom.us/j/97252910824)
	Session SatC5 - Intelligent Sensing and Safe Control System Technologies of Unmanned Aerial Vehicle Papers: 147, 176, 355, 435, 436, 439 (https://ntu-sg.zoom.us/j/95562539552)	**Session SatC6 - Nonlinear Control** Papers: 57, 69, 72, 91, 220, 423 (https://ntu-sg.zoom.us/j/94013707778)

DAY 3 (October 11, Sunday), Zoom Passcode: See Email Notice		
9:00-9:50 (Singapore time)	**Award Ceremony** (https://ntu-sg.zoom.us/j/91462345017) (https://meeting.tencent.com/s/wDou9FecLphw)	
10:00-11:40	**Plenary Panel Discussion Session, by Profs. Clarence W. de Silva, Wei Kang, Tong Boon Quek, Yacov A. Shamash, Bin Xin, and Chaired by Profs. Jie Chen and Ben M. Chen** **Topic: Autonomous Systems, AI and Commercialization Opportunities** (https://cuhk.zoom.us/j/97039359394) (https://meeting.tencent.com/s/VE8ClJZEhh2q)	
	Lunch Break	
13:00-14:30	**Session SunA1 - Robotic Manipulation and Coordination of Multi-Robot Systems** Papers: 202, 245, 303, 339, 354, 416 (https://ntu-sg.zoom.us/j/96783107921)	**Session SunA2 - On distributed control of multi-agent systems** Papers: 42, 63, 159, 161, 340, 388 (https://ntu-sg.zoom.us/j/96220596383)
	Session SunA3 - Sensing, Estimation, Control and Optimization for Networked Systems Papers: 177, 193, 223, 235, 255, 335 (https://ntu-sg.zoom.us/j/96429857632)	**Session SunA4 - Robotics 3** Papers: 134, 257, 366, 413, 415, 433 (https://ntu-sg.zoom.us/j/91967328904)
	Session SunA5 - Modeling, Control and Optimization of Cyber-Physical Systems Papers: 110, 113, 153, 205, 253, 319 (https://ntu-sg.zoom.us/j/95297276240)	**Session SunA6 - Recent Advances in Control of Networked Systems** Papers: 92, 106, 142, 170, 182, 299 (https://ntu-sg.zoom.us/j/97455636411)
14:45-16:15	**Session SunB1 - On Cyber-physical Systems: Control, Optimization and Security** Papers: 90, 132, 135, 155, 315 (https://ntu-sg.zoom.us/j/94926726246)	**Session SunB2 - Recent advances on distributed control and optimization methods for networked systems** Papers: 129, 130, 141, 151, 274, 369 (https://ntu-sg.zoom.us/j/91537640115)
	Session SunB3 - Integrated Networked Control for Massively Many IoT Devices Papers: 187, 204, 229, 384, 419 (https://ntu-sg.zoom.us/j/92391155037)	**Session SunB4 - Unmanned Systems: Theory and Applications** Papers: 119, 181, 190, 275, 307 (https://ntu-sg.zoom.us/j/93651629908)
	Session SunB5 - Observation, Disturbance Rejection, and Learning for uncertain systems Papers: 143, 145, 330, 371, 381 (https://ntu-sg.zoom.us/j/96650156404)	**Session SunB6 - The Coordinated Control of Multi-Agent Systems** Papers: 84, 124, 296, 370, 379 (https://ntu-sg.zoom.us/j/92551965135)

2020 IEEE 16th International Conference on Control & Automation (ICCA)
Oct 9-11, 2020 (Virtual) Sapporo, Hokkaido, Japan

A Bi-bandwidth Extended State Observer for System with Measurement Noise

Lilei Liu, Lingyu Yang and Jing Zhang

***Abstract*— Although traditional Extended State Observer (ESO) can efficiently estimate the total disturbance of the system theoretically, observation may diverge from the actual system when the measurement noises exist, due to the sensibility of such high-gain-observer to noises. The trade-off between transient property and denoise capacity of ESO considerably complicates the tuning of gain parameters. Taking this into account, we proposed a novel ESO-based approach, the Bi-bandwidth ESO (BESO), which uses direction information of estimation error rate to tune the bandwidth of ESO dynamically. Numerical comparisons among the LESO, NESO, and BESO, are given to demonstrate the effectiveness of our proposed approach for tackling observation issues with measurement noises.**

I. INTRODUCTION

Because of the inaccurate model and various internal/external disturbances of practical physical systems, the performances of traditional control techniques requiring precise model may degrade, and the closed-loop system based on them may even fail[1]. To cope with this problem, employing model-free control techniques is of great importance, of which the Adaptive Disturbance Rejection Control (ADRC) is a typical one. Because of its easy deployment and considerable robustness, the last two decades have been witnessing the broad and successful application of ADRC in various industrial fields, such as DC-DC power converter[2], gasoline engines[3], and flight control systems[4], [5].

As a cardinal component of ADRC architecture, the elaborately designed and employed Extended State Observer (ESO) has gone beyond the category of ADRC into a general compensation technique. Just like ADRC having a model-free property, an ESO is also a model-free method (from which the model-free property of ADRC originates), which packs modeling uncertainty between nominal model and the actual system, and internal/external disturbances as a total disturbance without discrimination and estimates system state and total disturbance simultaneously. Generally speaking, the traditional ESO has two classes, namely Nonlinear and Linear ESO (resp. NESO and LESO). The difference between those two is mainly in the form of error feedback function.

In Han's monograph about ADRC[6], an NESO with a elaborately designed nonlinear error feedback function $\mathrm{fal}(\tau, \alpha, \delta)$ is proposed. A few qualitative parameter selection methods, such as the simulation-step-based method and the Fibonacci-sequence-based method, are discussed. A recent work gave a rigorous proof about the stability and convergence of NESO, then proposed a quantitative parameter selection strategy according to it [7]. This strategy guarantees the stability and convergence of NESO. However, the balance between transient performance and denoise capacity still is not discussed and remains an open issue. The calculation of various kinds of bounds brings additional labor for designers without making a deterministic difference to this object.

Although a NESO is more efficient than LESO[6], which can achieve as comparative performance as LESO with considerably low gain, the wider used ESO is still its linear counterpart because of humans' mind preferring sticking to a linear form. The error feedback functions in LESO degrades into a linear form. When talking about turning LESO, we refer to change the so-called bandwidth of it to adjust the characteristic equation to a preferred form $(s+\omega)^{n+1}$[8], which is also known as a high gain observer in other articles[9], [10], and the convergence of it is discussed in [11]. Except for the widely used bandwidth approach, a modification of LESO, the Adaptive ESO (AESO) proposed in [3], can dynamically alter the gains according to the noise covariance. The numerical example indicates that the bandwidth-based method maybe not optimal when measure noises exist. Also, an LMI-based L_2 observer gain design method is discussed in [12], which guarantees the upper bound of the ratio between 2-norms of unknown external input and estimation if the nonlinear dynamics of the plan satisfies the so-called incremental quadratic constrain[13]. However, such a robust approach may impact the transient property, and the denoise capacity is not mentioned in it.

In all those Luenberger-like observes, including LESO, a higher gain always brings a satisfying transient performance. However, since the measurement noise is omnipresent in any detect techniques, the noise mingled with the measurement can be amplified into a super high level. Nevertheless, if we try to choose a low gain to attenuate this amplification, we must sacrifice the transient property to some extent. Trying to find a balance between denoise capacity and transient property, a novel Bi-bandwidth ESO (BESO) is proposed in this paper, which is the main contribution of this paper.

The structure of this paper is as follows. Firstly, we introduce preliminaries and problems in section II, where the macro aspect of ESO is discussed. In section III, the BESO is proposed, and the existing approaches are also listed as comparisons, which is followed by a numerical example to demonstrate the effectiveness of it in section IV.

This work was supported by National Nature Science Foundation of China under Grant 61273099 and Grant 61304030

Authors are with School of Automation Science and Electrical Engineering, BeiHang University, XueYuan Road No.37, HaiDian District, BeiJing, China yanglingyu@buaa.edu.cn

TABLE I

COST FUNCTIONAL

estimation	state J_{e_s}	$\frac{1}{T}\int_0^T \|\|\boldsymbol{x} \quad \hat{\boldsymbol{x}}\|\|_2 \mathrm{d}t$
	disturbance J_{e_d}	$\frac{1}{T}\int_0^T \|\|\boldsymbol{f} \quad \hat{\boldsymbol{f}}\|\|_2 \mathrm{d}t$
tracking	J_{e_r}	$\frac{1}{T}\int_0^T \|\|\boldsymbol{x_c} \quad \boldsymbol{x_r}\|\|_2 \mathrm{d}t$

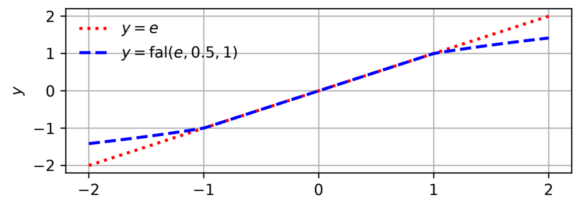

Fig. 1. Feedback functions of LESO and NESO

Furthermore, the conclusions in section V put an end to this article.

II. PROBLEM FORMULATION

Multiple Inputs and Multiple Outputs (MIMO) systems with parameter uncertainty, disturbance, and measurement noise can be formed as (1) and (2).

$$\dot{\boldsymbol{x}} = \boldsymbol{Ax} + \boldsymbol{Bu} + \underbrace{\Delta\boldsymbol{Ax} + \Delta\boldsymbol{Bu} + \boldsymbol{d}}_{\boldsymbol{f}}, \tag{1}$$

$$\begin{cases} \boldsymbol{x_s} = \boldsymbol{x} + \boldsymbol{n_x} \\ \boldsymbol{u_s} = \boldsymbol{u} + \boldsymbol{n_u} \end{cases}, \tag{2}$$

where $\boldsymbol{x} \in \mathbb{R}^n$ is the state vector, $\boldsymbol{u} \in \mathbb{R}^m$ refers to the input, $\boldsymbol{A}$ and $\boldsymbol{B}$ are matrices with proper shape. The model uncertainties are denoted as $\Delta\boldsymbol{A}$ and $\Delta\boldsymbol{B}$, while the disturbance is referred as $\boldsymbol{d} \in \mathbb{R}^m$, and $\Delta\boldsymbol{Ax}+\Delta\boldsymbol{Bu}+\boldsymbol{d}$ composes the so-called total disturbance $\boldsymbol{f}(\boldsymbol{x},\boldsymbol{u},\boldsymbol{d}) : \mathbb{R}^n \times \mathbb{R}^m \times \mathbb{R}^m \mapsto \mathbb{R}^n$. And we assume that state $\boldsymbol{x}$ can be measured but mingled with noise $\boldsymbol{n_x}$ and the actual measurement is $\boldsymbol{x_s}$, so as the input $\boldsymbol{u}$, noise $\boldsymbol{n_u}$ and $\boldsymbol{u_s}$, and $\boldsymbol{n_x}$ and $\boldsymbol{n_u}$ are white noises with known power.

The goal of this paper is to estimate the state $\boldsymbol{x}$ and total disturbance $\boldsymbol{f}$ in system (1) with an acceptable transient property when measurement noise exist. To evaluate the observer performance, we proposed cost functions J_{e_s} and J_{e_d}, listed in Table I, where $\hat{\boldsymbol{x}}$ and $\hat{\boldsymbol{f}}$ are the state and disturbance estimations by ESO. Because estimation is always for compensation in closed-loop system, except J_{e_s} and J_{e_d}, we propose J_{e_r} to evaluate the closed-loop tracking performance. The target trajectory is generated by a reference

$$\dot{\boldsymbol{x}}_r = \boldsymbol{Ax_r} + \boldsymbol{Br}, \tag{3}$$

where $\boldsymbol{x_r} \in \mathbb{R}^n$ denotes the reference state vector and $\boldsymbol{r}$ is the reference input vector. As for the coefficient matrix $\boldsymbol{B} \in \mathbb{R}^{n\times m}$, we assume that $n \geq m$ and $\mathrm{rank}(\boldsymbol{B}) = m$. And $\boldsymbol{x_c}$ is the trajectory of closed-loop system with the compensation input $\boldsymbol{u} = \quad (\boldsymbol{B^T B}) \ ^{1}\boldsymbol{B^T}\hat{\boldsymbol{f}} + \boldsymbol{r}$.

III. THE BI-BANDWIDTH EXTENDED STATE OBSERVER

In this section, the novel BESO is proposed. Firstly, we analyze traditional ESO.

To make a system defined in (1) tracking the reference one as (3), a straightforward strategy is to estimate the disturbance $\boldsymbol{f}(\boldsymbol{x},\boldsymbol{u},\boldsymbol{d})$ and compensate it with proper input. Therefore, how to precisely estimate the total disturbance is of considerable importance, a preciser estimation always guarantees a better tracking performance (though they are not equal, as shown in section IV). Generally speaking, we can take a two-step schedule to achieve our goal, namely estimation, then compensation. We will concentrate on two mainstream ESO-based estimation approaches, namely LESO, NESO, and their enhanced BESO in the following, and the compensation method is discussed when forming a closed-loop system.

Firstly, we concentrate on the LESO.

$$\begin{cases} e_i = x_{s_i} - \hat{x}_i \\ \dot{\hat{x}}_i = \boldsymbol{A_i}\hat{\boldsymbol{x}} + \boldsymbol{B_i u} + \hat{f}_i + \beta_i e_i \\ \dot{\hat{f}}_i = \beta_{i+n} e_i \end{cases} \tag{4}$$

where e_i is the difference between estimation $\hat{x}_i$ and measurement x_{s_i}, $\hat{x}_i$ and $\hat{f}_i$ are estimations of x_i and f_i respectively, and β_i and β_{i+n} are gains of the LESO feedback functions. When we use a bandwidth-based method to design those gains, they have the following form,

$$\beta_i = 2\omega_i, \;\; \beta_{i+n} = \omega_i^2, \tag{5}$$

in which the ω_i is the so-called bandwidth of the $\mathrm{i^{th}}$ subsystem. As we can see, the gain has a power growth property w.r.t. bandwidth. Otherwise, if we choose a LMI-based method, the gains are calculated via solving LMIs, or if we choose the so-called AESO method, the gains are updated according to the measurement rather than given initially yet converge quickly[3].

Essentially, NESO is an extension of LESO, which usually introduces more parameters, its structure are as following,

$$\begin{cases} e_i = x_{s_i} - \hat{x}_i \\ \dot{\hat{x}}_i = \boldsymbol{A_i}\hat{\boldsymbol{x}} + \boldsymbol{B_i u} + \hat{f}_i + \beta_i h_i(e_i) \\ \dot{\hat{f}}_i = \beta_{i+n} h_{i+n}(e_i) \end{cases}, \tag{6}$$

where $h_i(\cdot)$ and $h_{i+n}(\cdot)$ are functions w.r.t. e_i, if they are linear, Equation (6) degrades to a LESO. The wide use nonlinear feedback function has the following form,

$$\mathrm{fal}(e,\alpha,\Delta) = \begin{cases} \dfrac{e}{\Delta^{1-\alpha}}, & |e| \leq \Delta, \\ |e|^\alpha \mathrm{sign}(e), & |e| > \Delta. \end{cases}, \tag{7}$$

where $\alpha < 1$. The function defined in (7) is linear in interval $[-\Delta,\Delta]$ and is nonlinear when $|e| > \Delta$. And their shape is depicted in Fig. (1).

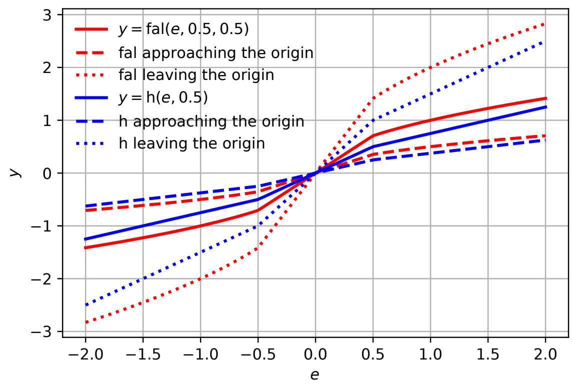

Fig. 2. Feedback functions and bi-bandwidth modifications

When employing observer-based approaches, the estimation and tracking errors are composed of two ingredients, namely lag (which brings extensive error yet in a short period) and measurement noises (which consistently affect the system yet are relatively small). However, their contributions vary in different periods. Lag plays a major role when the system intensively varies, such as abrupt strong disturbance injection, while noise contributes a lot when the system is steady. As is shown in Fig. (1), when estimation error $e > \Delta$, the gain of $\mathrm{fal}(e, 0.5, 1)$ is less than the linear function's, and when the system is steady, the nonlinear and linear functions are equivalent given β_is both chosen via bandwidth-based method.

Usually, we chose a wide bandwidth to suppress the lag, which means the gains are relatively high. As a consequence, any noise mingled with the actual signal would be amplified to a considerably high level. However, if we want to attenuate this phenomenon by choosing a narrow bandwidth, the lag may then become a significant problem. It is complicated to find a balance even in such an open-loop situation.

To solve the trade-off between transient property and de-noise capacity of traditional ESO approach, the BESO is proposed. Firstly, the Bi-bandwidth Linear Extended State observer (BLESO) is given as

$$\begin{cases} e_i = x_{s_i} - \hat{x}_i \\ \gamma_i = \delta_i^{-\mathrm{sign}(\frac{d|e_i|}{dt})} \\ \dot{\hat{x}}_i = \boldsymbol{A_i}\hat{\boldsymbol{x}} + \boldsymbol{B_i}\boldsymbol{u} + \hat{f}_i + \beta_i\gamma_i e_i \\ \dot{\hat{f}}_i = \beta_{i+n}\gamma_i^2 e_i \end{cases}, \tag{8}$$

Where the direction information of the estimate error rate is introduced in the observer via γ_i, which is cardinal to achieve a bi-bandwidth observer. The feedback function of BLESO has a unique bi-bandwidth nonlinear characteristic.

Such a method can be applied to the NESO easily and then form a Bi-bandwidth Nonlinear Extended State Observer (BNESO),

$$\begin{cases} e_i = x_{s_i} - \hat{x}_i \\ \gamma_i = \delta_i^{-\mathrm{sign}(\frac{d|e_i|}{dt})} \\ \dot{\hat{x}}_i = \boldsymbol{A_i}\hat{\boldsymbol{x}} + \boldsymbol{B_i}\boldsymbol{u} + \hat{f}_i + \beta_i\gamma_i h_i(e_i) \\ \dot{\hat{f}}_i = \beta_{i+n}\gamma_i^2 h_{i+n}(e_i) \end{cases}. \tag{9}$$

When we chose $h(\cdot)$ as $\mathrm{fal}(e, 0.5, 0.5)$, function $\gamma h(e)$ is shown in Fig. (2). In our numerical simulation, a piecewise linear function will be employed as $h(\cdot)$, which has the following property

$$\frac{\mathrm{d}h(e,\Delta)}{\mathrm{d}e} = \begin{cases} k, & |e| \le \Delta \\ \epsilon k, & |e| > \Delta \end{cases} \tag{10}$$

where k is designed via bandwidth-based method, $0 < \epsilon < 1$ and Δ is the breakpoint. Nonlinear function $\mathrm{h}_i(\cdot)$ has a similar curve like $\mathrm{fal}(\cdot)$ which is also given in Fig. (2). When error approaches or leaves the origin, slopes of lines are different, after which the bi-bandwidth is named. However, neither linear function nor nonlinear ones used in traditional ESO have such a property, which are both one-to-one mappings from error to the output.

The proposed BESO approach has the following properties:

1) A bi-bandwidth term γ_i is introduced in the feedback function of BESO, which brings additional information to the observer, i.e., the direction of the estimated error rate. Consequently, the proposed BSEO may be more efficient than traditional ESO.

2) When $\delta_i = 1$, the BESO is equivalent to the traditional ESO. Therefore, our bi-bandwidth ESO is an extension of the traditional ones.

3) In case of $\delta_i \neq 1$, the proposed BESO has a so-called bi-bandwidth property, i.e., when error directs to the origin, the bandwidth of it is $\beta_i\delta_i/2$, otherwise $\beta_i/2\delta_i$. In particular, for a system with measurement noise, a BESO with $\delta_i < 1$ outperforms one with $\delta_i > 1$, and our discussion below is based on the former case.

Dig deeper and make a comparison; we can find the underlying mechanism of BESO. After the bi-bandwidth modification being introduced, when error leaves the origin, the bi-bandwidth function provides high gains to guarantee the transient property. However, it alters to a low gain to suppress the impact of measurement noise when error approaches the origin. As is shown in Fig. (1), the feedback function of NESO preferred a low gain when error crosses the linear bound, which is believed to make NESO more efficient than LESO. However, our approach goes beyond this. The feedback functions use the direction information of error rate to provide a better adaptation to gains, which may be why our approach is more effective than the traditional ones.

Since we already get the precise estimation about $\boldsymbol{f}(\boldsymbol{x}, \boldsymbol{u}, \boldsymbol{d})$, then the control strategy is straightforward as mentioned in the earlier discussion of cost functions. Because we already assume that the coefficient matrix $\boldsymbol{B}$ is full column rank, a input signal, such as $\boldsymbol{u} = (\boldsymbol{B}^T\boldsymbol{B})^{-1}\boldsymbol{B}^T\hat{\boldsymbol{f}} + \boldsymbol{r}$, is straightforward to compensate the disturbance and track the reference (3).

IV. NUMERICAL EXAMPLE

Consider a MIMO system as (1), where

$$\boldsymbol{A} = \begin{bmatrix} -5 & 1 & 1 \\ -1 & 5 & 1 \\ 0 & 0 & -1 \end{bmatrix}, \boldsymbol{B} = \boldsymbol{I}_3, \boldsymbol{C} = \boldsymbol{I}_3,$$

and

$$\boldsymbol{d} = \begin{bmatrix} \sin(0.1t) + 0.5 \\ -\sin(0.1t + 0.5) - 0.3 \\ 0.8\sin(0.1t - 0.5) + 0.2 \end{bmatrix} + \begin{bmatrix} 1.5\sin(0.04t + 0.5) + 1 \\ 0.3\sin(0.03t + 0.3) + 0.5 \\ -0.4\sin(0.05t - 0.2) + 0.3 \end{bmatrix} + \begin{bmatrix} 3\theta(t-5) \\ -9\theta(t-10) \\ 4.5\theta(t-15) \end{bmatrix},$$

in which

$$\theta(\tau) = \begin{cases} 0, & \tau < 0 \\ 1, & \tau \geq 0 \end{cases}.$$

The model uncertainties $\Delta\boldsymbol{A}$ and $\Delta\boldsymbol{B}$ are normal distributed random matrices with the proper shape, for simulation consistency, we randomly chose the following values for them,

$$\Delta\boldsymbol{A} = \begin{bmatrix} -0.3296 & -0.4260 & 0.4828 \\ -0.2422 & 0.1841 & -0.0978 \\ -0.1032 & -0.0976 & 0.1207 \end{bmatrix},$$

$$\Delta\boldsymbol{B} = \begin{bmatrix} -0.1037 & 0.0774 & 0.0557 \\ -0.0356 & 0.1113 & -0.0618 \\ -0.1017 & -0.0448 & 0.0092 \end{bmatrix}.$$

And the power of white noises $\boldsymbol{n_x}$ and $\boldsymbol{n_u}$ is 0.01^2.

The aforementioned ESO-based approaches, LESO and NESO, and their corresponding BESO methods are used to estimate and compensate the total disturbance in the actual system defined in (1), and design proper control strategy which ensures the actual system tracking the reference one.

At first, we will focus on the LESO approach. After a coarse search, we find that the ESO with bandwidth $\omega = 17$ rad/s has a preferred performance in our search area. In order to depict the trade-off between transient property and denoise capacity, we chose $\omega = 9, 17$ and 25 rad/s as examples. The estimation errors of the second component of $\boldsymbol{f}$ are given in Fig. (3).

It's obvious that greater bandwidth we chose, a shorter lag period lasts, yet a higher level of noise amplification exists. The costs are calculated in Table II. As aforementioned, a preciser estimation is not equivalent to a better tracking, it is shown that when $\omega = 17$ rad/s the estimation about disturbance is much preciser than $\omega = 25$ rad/s, but the closed-loop tracking performance of the latter is better with the index discussed here.

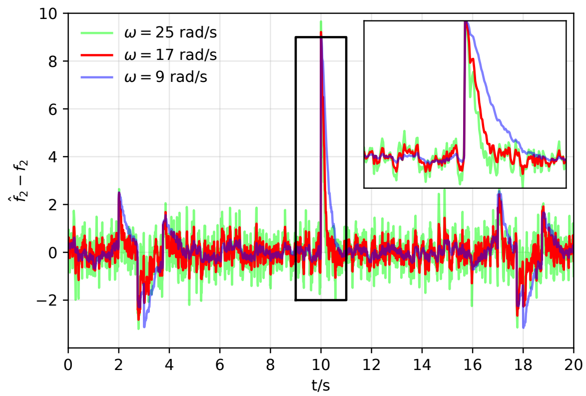

Fig. 3. Estimation errors of f_2 by LESO with various bandwidth

According to the above analysis, we find that it is hard to find a compromise between transient property and steady state noise attenuation. Then we have made a comparison between LESO and the proposed BLESO, and the estimation and tracking errors of BLESO ($\delta = 0.4, \omega = 17$ rad/s) and the preferred LESO ($\omega = 17$ rad/s) are given in Table IV, and the results are shown in Fig. 4

Comparing with the LESO, J_{e_r} is reduced considerably. For example, when 10 s $< t < 11$ s, the total disturbance f_2 intensively varies, and the LESO is relatively slow to track it. However for the BLESO approach, the lag is suppressed, and the noise amplification is acceptable. When $t = 10$s, a jump is introduced into f_2, the transient process of BLESO is faster than traditional ones, yet has far less noise amplification. These facts demonstrate that our bi-bandwidth strategy is effective in the LESO scenario, which can achieve a better transient property and maintain a considerable denoise capacity in the meanwhile.

In the following, we will demonstrate the bi-bandwidth modification can be introduced into NESO to further improvements on system performances. A preferred NESO have the following parameters

$$\beta_1 = 2 \times 17, \epsilon_1 = 0.7, \beta_2 = 17^2, \epsilon_2 = 0.7^2, \Delta = 0.25.$$

It's shown that the NESO has same bandwidth $\omega = 17$ rad/s, with the LESO discussed above, which indicates that when the closed-loop system is steady, actual error maybe bounded in $[-0.25, 0.25]$. If we change Δ, costs remain similar to

TABLE II
COST VALUES OF LESO

bandwidth (rad/s)	estimation		tracking
	J_{e_s}	J_{e_d}	J_{e_r}
$\omega = 9$	0.0618	0.9187	0.2077
$\omega = 13$	0.0590	0.7609	0.1478
$\boldsymbol{\omega = 17}$	**0.0637**	**0.7557**	**0.1158**
$\omega = 21$	0.0698	0.8438	0.0966
$\omega = 25$	0.0758	0.9870	0.0846

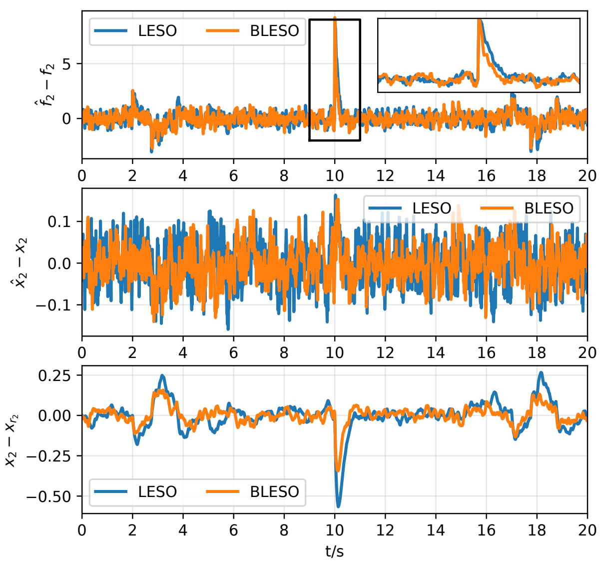

Fig. 4. Estimation errors of f_2 and x_2, tracking errors of x_{r_2} with LESO and BLESO approaches

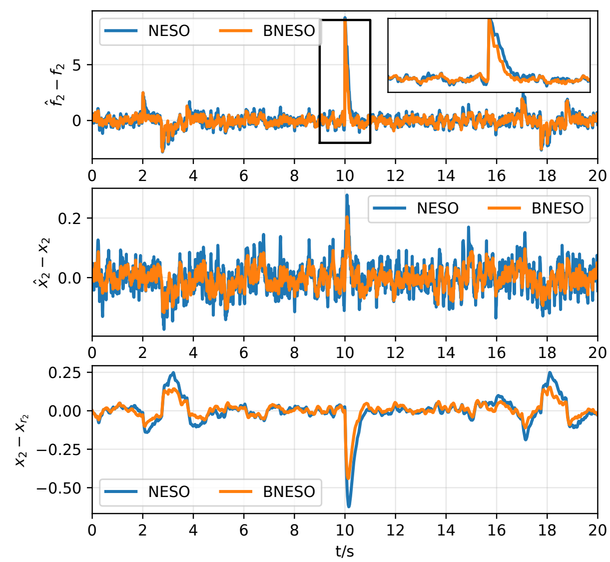

Fig. 5. Estimation errors of f_2 and x_2, tracking errors of x_{r_2} with NESO and BNESO approaches

each other, which is indicated in Table III when $\omega = 17$ rad/s and $\epsilon = 0.7$. However, a different bandwidth may affect the closed-loop system a lot. A few of costs are also given in Table III when $\Delta = 0.25$ and $\epsilon = 0.7$.

The estimation errors of f_2, x_2 ,and tracking error of x_{r_2} with the optimal NESO are shown in Fig. (5). Also we find a bi-bandwidth modified NESO with piece-wise linear feedback function with the following parameters preferred in our search region

$$k_1 = 2 \times 10, k_2 = 10^2, \Delta = 0.15, \epsilon = 0.2, \delta = 0.3.$$

Error trajectories of the closed-loop system are also given in Fig. 5. As is shown in Fig. (5). If we use the estimation of total disturbance of NESO as compensation, the closed-loop system has a deviation from reference at time $t = 10$s, the value of which is about 0.65. However, in the BNESO case, which is also shown in Fig. (5), the value is about 0.44, above a 30% reduction.

Costs of optimal LESO, BLESO, NESO, and BNESO in our search region, is given in Table IV. It's shown that the bi-bandwidth based LESO and NESO have considerable advantages comparing with traditional ones. Particularly, the newly proposed BESO is very efficient, which can achieve a preferred transient property via a relatively low gain and suppress the measurement noise amplification to some extend.

TABLE III
NESO WITH DIFFERENT BREAK POINT AND BANDWIDTH

break point	bandwidth (rad/s)	estimation		tracking
		J_{e_s}	J_{e_d}	J_{e_r}
$\Delta = 0.25$	$\omega = 17$	0.0637	0.7558	0.1157
$\Delta = 0.27$	$\omega = 17$	0.0637	0.7559	0.1157
$\Delta = 0.29$	$\omega = 17$	0.0637	0.7558	0.1157
$\Delta = 0.25$	$\omega = 15$	0.0610	0.7441	0.1297
$\Delta = 0.25$	$\omega = 17$	0.0637	0.7558	0.1157
$\Delta = 0.25$	$\omega = 19$	0.0667	0.7905	0.1050

TABLE IV
COSTS OF ESO-BASED APPROACHES

approach	estimation		tracking
	J_{e_s}	J_{e_d}	J_{e_r}
LESO	0.0637	0.7557	0.1158
BLESO	**0.0580**	**0.7579**	**0.0794**
NESO	0.0637	0.7558	0.1157
BNESO	**0.0445**	**0.5306**	**0.0749**

V. CONCLUSION

In this paper, we proposed a novel ESO approach called bi-bandwidth ESO, which is easily implemented and has the so-called bi-bandwidth property. The ESO-based tracking problem of a MIMO system with matched total disturbance discussed above shows that the BESO-based approach employed in our model strikes a balance between the transient property and de-noise capacity to some extent, as we have expected. Intuitively, when we introduce error direction information to tune the bandwidth or gain of ESOs dynamically, we do not change the sign of error feedback functions. Therefore, we believe the stability can be guaranteed. The vigorous analysis of stability and performance improvement of BESO is our future focus.

REFERENCES

[1] Michael Green, D.J.N. Limebeer, *Linear Robust Control*, Prentice-Hall, Englewood Cliffs, NJ; 1995.

[2] Bosheng Sun, Zhiqiang Gao, "A dsp-based active disturbance rejection control design for a 1-kwh-bridge dc-dc power converter", *IEEE Transactions on Industrial Electronics*, Vol. 52, 2005, pp 1271-1277.

[3] Wenchao Xue, Wenyan Bai, Sheng Yang, Kang Song, Yi Huang, Hui Xie, "Adrc with adaptive extended state observer and its application to air-fuel ratio control in gasoline engines", *IEEE Transactions on Industrial Electronics*, Vol. 62, 2015, pp 5847-5857.

[4] J Zhang, J Yan, L Yang, Y Mou, "Robust IFNTSM–ESO Control Design for Aircraft Subject to Parameter Uncertainties.", *International Journal of Aeronautical and Space Sciences*, 2019, pp 1-12.

[5] J Zhang, X Xu, L Yang, X Yang, "LPV Model-Based Multivariable Indirect Adaptive Control of Damaged Asymmetric Aircraft."*Journal of Aerospace Engineering*, Vol. 32, 2019, pp 04019095.

[6] Jinqing Han, *Adaptive Disturbance Rejection Control Technique*, National Defense Industry Press, Beijing; 2008.

[7] Zhi-Liang Zhao, Bao-Zhu Guo, "A nonlinear extended state observer based on fractional power functions", *Automatica*, Vol. 81, 2017, pp 286-296.

[8] Zhiqiang Gao, "Scaling and bandwidth-parameterization based controller tuning", Vol. 6, 2003, pp 4989-4996.

[9] Leonid B Freidovich, Hassan K Khalil, "Performance recovery of feedback-linearization-based designs", *IEEE Transactions on Automatic Control*, Vol. 53, 2008, pp 2324-2334.

[10] Laurent Praly, Zhongping Jiang, "Linear output feedback with dynamic high gain for nonlinear systems", *Systems & Control Letters*, Vol. 53, 2004, pp 107-116.

[11] Qing Zheng, L.Q. Gao, Zhiqiang Gao, "On stability analysis of active disturbance rejection control for nonlinear time-varying plants with unknown dynamics", *2007 46th IEEE Conference on Decision and Control*, New Orleans, LA, 2007, pp. 3501-3506.

[12] Martin Corless, Ankush Chakrabarty, "L_2 observers for a class of nonlinear systems with unknown inputs", *European Control Conference 2019*, Naples, 2019.

[13] Behcet Acikmese and M Corless. "Observers for systems with nonlinearities satisfying incremental quadratic constraints", *Automatica*, Vol. 47, 2011, pp 1339-1348.